Measurement of the gradient of viscosity with composition of gas mixtures at low temperatures .

P. A. Russell[†], B. A. Buffham, G. Mason, K. Hellgardt
Department of Chemical Engineering, Loughborough University,
Loughborough, Leicestershire LE11 3TU, England

Abstract
A perturbation viscometer is a differential capillary viscometer that measures the logarithmic viscosity gradient of the viscosity-composition curve for gas mixtures. Both the flow and composition of a gas mixture flowing through a capillary tube are perturbed by the addition of a small flow of gas (normally one of the pure components of the gas mixture). Pressure changes are seen at the capillary due to the change in flowrate and the change in viscosity. A delay line installed between the pertubation addition valve and capillary separates these pressure changes hence the capillary act first as a laminar flow meter and then as a viscometer. The logarithmic viscosity gradient can be calculated from the ratio of these pressure changes. Measurements are made at different gas mixture compositions. Integration of the logarithmic viscosity gradients measured over the full composition range gives the mixture viscosity relative to the viscosity of one of the pure components of the gas mixture. This method is attractive because, for measurements of equal precision integration of the *gradients* is potentially an order of magnitude more precise than measurement of the viscosities directly. It can also work at high and low temperatures and perhaps high pressures.

Previously the perturbation viscometer has been used to make measurements on ideal gas mixtures at ambient and elevated temperatures. The situation is more complicated when the gas mixtures are non-ideal. Here we describe a new apparatus optimised to make viscosity measurements for non-ideal gas mixtures in the temperature range –30 to +50˚C. We show how simple modifications to the perturbation viscometer have been made which permit the molar volume change on mixing and temperature effects of non-ideal gas behaviour to be separated out as additional pressure steps. To complement the new apparatus a refined theory of operation is presented which compensates for these non-ideal gas effects.

The apparatus has been tested using helium–pentafluoroethane mixtures and two new vicosity–composition profiles are presented for the temperatures 23˚C and –23˚C. Internal consistency tests have been used confirm that the data produced are of high quality.

Introduction

Perturbation viscometry is a recently established method developed to complement more conventional measurement techniques i.e capillary and oscillating body viscometry (See Toloukian (1975)). Perturbation viscometry measures a gradient of the viscosity-composition function. If viscosity gradients are known across the composition range then integration of these gradients gives viscosity values across the composition range relative to one of the pure components.

The method has been used previously to make viscosity measurements on mixtures of ideal gases at ambient temperature and pressure (see Heslop et al., (1996), (1998) and Mason et al., (1998)). The definitive design of a perturbation viscometer for ideal gas mixtures was reported Russell et al (2003)a.

This paper reports the development of the Russell et al (2003)a apparatus to make measurements on non-ideal mixtures. A simplified schematic drawing of the new apparatus is shown in Figure 1 and a typical pressure record for an experiment is given as Figure 2. A typical experimental run performed on the new apparatus starts with a main molar flow M of gas of composition X_i^0 passing through valve 2, the ambient temperature delay line, next a cold delay line and finally the measuring capillary. Valve 1 can deliver a small flow of gas of composition X_i^0 or a small flow of perturbation gas of composition X_i^T. Valve 2 can deliver either of these streams into the main flow or into a purge stream at the same conditions as the main experimental flow. When the X_i^0 stream is used this arrangement fills the transfer line between the two valves with gas of composition X_i^0.

Valves 1 and 2 are switched simultaneously. The volume of gas in the transfer line composition X_i^0 is pushed in the main flow causing an increase in flow with out a change in composition and the pressure rise P_1-P_0 is observed. The gas in the transfer line is pushed as a 'slug' of gas into the main flow but with the volumetric flow of the perturbation stream X_i^Tafter about 1 minutes duration. The composition of the perturbation flow being added to the main flow then changes to X_i^T. The volume of gas in the system changes as the main flow and perturbation flow mix and this causes the pressure change P_2-P_1. After a short time the composition front enters the cold block and is cooled. Pressure change P_3-P_2. is observed due to the difference between the thermal expansivities of the two gas streams. Finally the composition front reaches the measuring capillaries and the pressure change P_4-P_3 occurs because of the change in viscosity of the gas present in the capillary tube. Note that due to the dispersion in the delay lines the later viscosity pressure steps are not as abrupt as the first.

The perturbation flow is removed by switching valves 1 and 2 simultaneously. Pressure P_5-P_3 corresponds to the reduction in flow when the perturbation flow is cut off. After a short delay the gas composition in the cold delay line changes back to X_i^0 and pressure change P_6-P_5 is observed due to the change in thermal expansivity of the gas. P_7-P_6 is observed when the gas in the capillary returns to its initial composition and viscosity. It is important to note when the perturbation is removed no pressure change due to volume of mixing are observed.

Theory

The pressure changes shown in Figure 2 are conventionally used as nondimensional ratios. For non-ideal gas mixtures these ratios are defined as :-
For adding the perturbation flow

$$R_1 = \frac{P_2 - P_1}{P_1 - P_0} = \frac{\text{Change in molar volume of gas mixture on mixing}}{\text{flow of perturbation gas}} \qquad 1$$

$$R_2 = \frac{P_3 - P_2}{P_1 - P_0} = \frac{\text{Change in thermal expansion of gas mixture}}{\text{flow of perturbation gas}} \qquad 2$$

$$R_3 = \frac{P_4 - P_3}{P_1 - P_0} = \frac{\text{Change in thermal expansion of gas mixture}}{\text{flow of perturbation gas}} \qquad 3$$

and for removing the perturbation flow

$$R_4 = \frac{P_6 - P_5}{P_5 - P_4} = \frac{\text{Change in thermal expansion of gas mixture}}{\text{flow of perturbation gas}} \qquad 4$$

$$R_5 = \frac{P_7 - P_6}{P_5 - P_4} = \frac{\text{Change in viscosity of gas mixture}}{\text{flow of perturbation gas}} \qquad 5$$

For infinitesimal perturbation flows ratios R_1 and R_5 both equal the gradient of the viscosity-composition curve $\frac{\mathrm{d}\ln\mu}{\mathrm{d}X_i}$. In reality R_1 and R_5 are not equal because perturbations have a small finite size which cannot be ignored.

Calculation of viscosity gradients from small perturbation flows for non ideal gas mixtures

When making measurements we are considering the transition from point (X_i, μ) to point ($X_i+\Delta X$, $\mu+\Delta\mu$) and measuring the gradient of the chord between them. It can be shown that this gradient is equal to the slope of the $\ln\mu$ against X_i curve at the midpoint of the composition interval (Russell et al 2003a). For small finite perturbations the gradient of this chord is calculated as a power series expansion in $\frac{\Delta\mu}{\mu}$ of the logarithm viscosity gradient

$$\frac{\Delta\ln\mu}{\Delta X_i} = \frac{\Delta\mu}{\mu\Delta X_i}\left(1 - \frac{1}{2}\frac{\Delta\mu}{\mu} + \frac{1}{3}\left(\frac{\Delta\mu}{\mu}\right)^2 - \frac{1}{4}\left(\frac{\Delta\mu}{\mu}\right)^3 + \ldots.\right) \qquad (5)$$

The power series can be truncated after the second term because all subsequent terms are very small. It contains two separate terms, $\frac{\Delta\mu}{\mu}$ the viscosity ratio and $\frac{1}{\Delta X_i}$ the composition variable which can be determined from the experimental results.

The expression for $\frac{\Delta\mu}{\mu}$

The expressions for $\frac{\Delta\mu}{\mu}$ is found by a detailed examination of the pressure changes across the measuring capillaries. The apparatus is run in the laminar flow regime hence Poiseuille's equation maybe used to describe the pressure differences observed across the measuring capillary. For isothermal operation at time zero, before the perturbation is added, the equation for the pressure difference across the down stream capillaries is :

$$P_0 - P_d = k_d \mu Q \tag{6}$$

Where k_d is a constant m is the viscosity and Q is the volumetric flowrate
For the flow change on addition of the perturbation flow this pressure difference it becomes :

$$P_1 - P_d = k_d \mu (Q + q) \tag{7}$$

when the perturbation gas and main flow mix the flowrate changes by Δq_1 and it becomes :

$$P_2 - P_d = k_d \mu (Q + q + \Delta q_1) \tag{8}$$

A second flow change Δq_2 is produced by the difference in thermal expansivity when the new gas composition enters the cold delay line and the equation becomes

$$P_3 - P_d = k_d \mu (Q + q + \Delta q_1 + \Delta q_2) \tag{9}$$

finally when the viscosity change is detected the pressure difference becomes :

$$P_4 - P_d = k_d (\mu + \Delta\mu)(Q + q + \Delta q_1 + \Delta q_2) \tag{10}$$

When the flow is removed the term $(q + \Delta q_1 + \Delta q_2)$ will disappear but a term Δq_3 must be included to account for the change in thermal expansivity when the composition front enters the cold region. Thus when the flow is removed the pressure difference thus becomes

$$P_5 - P_d = k_d (\mu + \Delta\mu)(Q + \Delta q_3) \tag{11}$$

when the composition front reaches the cold block Δq_3 disappears and it becomes

$$P_6 - P_d = k_d (\mu + \Delta\mu)(Q) \tag{12}$$

when the composition change reaches the measuring capillary it returns to the initial conditions

$$P_7 - P_d = k_d \mu (Q) \tag{13}$$

Algebraic manipulation of equations 6, 7 and 8 can be used to give an expression for R_1

$$R_1 = \frac{P_2^2 - P_1^2}{P_1^2 - P_0^2} = \frac{kd\mu(Q + q + \Delta q_1) - kd\mu(Q + q)}{kd\mu(Q + q) + kd\mu(Q)} \tag{14}$$

Rearrangement of equation 12 will give an expression for Δq_1

$$\Delta q_1 = R_1 q \tag{15}$$

a similar approach may be adopted to produce an equation for Δq_2

$$\Delta q_2 = R_2 q \tag{16}$$

Algebraic manipulation of equations 6, 7 ,9 and 10 gives a slightly different expression for R_3

$$R_3 = \frac{P_2^2 - P_1^2}{P_1^2 - P_0^2} = \frac{kd(\mu + \Delta\mu)(Q + q + \Delta q_1 + \Delta q_2) - kd\mu(Q + q + \Delta q_1 + \Delta q_2)}{kd\mu(Q + q) + kd\mu(Q)} \tag{17}$$

on rearrangement this gives

$$\frac{\Delta\mu}{\mu} = \frac{R_3 q}{Q + q + \Delta q_1 + \Delta q_2} \tag{18}$$

The flow changes caused by gas mixing and thermal expansion Δv_1 and Δv_2 are removed by substitution of equations 15 and 16 into equation 18. Thus for adding the perturbation flow

$$\frac{\Delta\mu}{\mu} = \frac{R_3}{\frac{Q}{q} + 1 + R_1 + R_2} \tag{19}$$

A similar approach is adopted for removing the perturbation flow. Δq_3 is calculated from

$$\Delta q_3 = q\frac{R_4}{(1 + R_4)}(1 + R_1 + R_2) \tag{20}$$

and the equation for $\frac{\Delta\mu}{\mu}$ becomes

$$\frac{\Delta\mu}{\mu} = \frac{R_5\left(1 - \frac{R_4}{(1 + R_4)}\right)(1 + R_1 + R_2)}{\frac{Q}{q} - R_5\left(1 - \frac{R_4}{(1 + R_4)}\right)(1 + R_1 + R_2)} \tag{21}$$

The expression for the composition term $\frac{1}{\Delta X_i}$

The second term required to solve the power series expansion (eq. 5) is the composition term $\frac{1}{\Delta X_i}$. This term is found by performing a mass balance across the perurbation valve

$$M(X_i^0) + m(X_i^T) = (M + m)(X_i^0 + \Delta X_i) \tag{22}$$

Rearrangement of equation 31 gives the expression for $\frac{1}{\Delta X_i}$

$$\frac{1}{\Delta X_i} = \frac{(M+m)}{m}\frac{1}{(X_i^T - X_i^0)} \tag{23}$$

The molar flows are obtained from the volumetric flows and molar volumes $\overline{V}^0$ & $\overline{V}^T$

$$\frac{1}{\Delta X_i} = \left(\frac{Q}{q}\frac{\overline{V}^T}{\overline{V}^0} + 1\right)\frac{1}{(X_i^T - X_i^0)} \tag{24}$$

The molar volumes for the pure components are required from alternative sources. The molar volume of the mixture $\overline{V}^0$ can be found from pressure ratio R_1 (see Russell et al 2003c). For most cases $\frac{\overline{V}^T}{\overline{V}^0}$ is virtually equal to unity.

Now the final goal equations for calculating the viscosity gradients can be defined these are

$$\frac{\Delta \ln \mu}{\Delta X_i} = \frac{1}{(X_i^T - X_i^0)}\left(\frac{Q}{q}\frac{\overline{V}^T}{\overline{V}^0} + 1\right)\left(\frac{R_3}{\frac{Q}{q} + 1 + R_1 + R_2}\right)\left(1 - \frac{1}{2}\frac{R_3}{\frac{Q}{q} + 1 + R_1 + R_2}\right) \tag{25}$$

And for removing the perturbation flow

$$\frac{\Delta \ln \mu}{\Delta X_i} = \frac{\left(\frac{Q}{q}\frac{\overline{V}^T}{\overline{V}^0} + 1\right)}{(X_i^T - X_i^0)}\left(\frac{R_5\left(\frac{R_4}{(1+R_4)} - 1\right)(1 + R_1 + R_2)}{\frac{Q}{q} - R_5\left(\frac{R_4}{(1+R_4)} - 1\right)(1 + R_1 + R_2)}\right)\left(1 - \frac{1}{2}\frac{R_5\left(\frac{R_4}{(1+R_4)} - 1\right)(1 + R_1 + R_2)}{\frac{Q}{q} - R_5\left(\frac{R_4}{(1+R_4)} - 1\right)(1 + R_1 + R_2)}\right) \tag{26}$$

Theory for calculation of relative viscosities directly from the large perturbation data.

The viscometer can be operated using large perturbation flows to permit viscosity ratios to be obtained directly from the measurements. For viscosity ratios for the mixture A–B a main flow of component A is taken and perturbation flow, increased from 1% to 100 % of the main gas flowrate, of gas B are added to it. By increasing the perturbation flow the vicosity change is measured for different compositions (see Figure 3). For example if a perturbation flow equal to the main flow of gas is used the viscosity change to the centre of the composition range is measured. To convert the pressure differences for large perturbations into viscosity ratios use is made of the definition of the viscosity change i.e.

$$\frac{\mu_{\text{mix}}}{\mu} = 1 + \frac{\Delta\mu}{\mu} \tag{27}$$

equations 19 and 21 provide expressions for $\frac{\Delta\mu}{\mu}$ in terms of the pressure ratios for adding and removing the perturbation flow respectively substitution of the equations into equation 27 give:
for adding the perturbation flow

$$\frac{\mu_{\text{mix}}}{\mu} = 1 + \frac{R_3}{\frac{Q}{q} + 1 + R_1 + R_2} \tag{28}$$

and removing the perturbation flow

$$\frac{\mu_{\text{mix}}}{\mu} = 1 + \frac{R_5\left(\frac{R_4}{(1+R_4)} - 1\right)(1 + R_1 + R_2)}{\frac{Q}{q} - R_5\left(\frac{R_4}{(1+R_4)} - 1\right)(1 + R_1 + R_2)} \tag{29}$$

The viscosity ratios obtained from small perturbations are calculated by the integration of the viscosity gradients measured at different compositions. The viscosity ratios measured using large perturbations are calculated directly but the increases in precision achieved by integration are lost. Viscosity ratios calculated from large perturbation flows are more susceptable to errors produced by:turning down the main flow M because the pressure drop across the upstream flow setting block is reduced due to the large increase in pressure at the upstream end of the measuring capillary; end effects on the measuring capillary; entrance length effects on the measuring capillary; compression effects within the measuring capillary; non parabolic flow in the helical coils of the capillary.

These effects can be compensated for but each correction will introduce errors into the viscosity ratio. The small perturbation method is therefore the preferred method of operation. The large perturbation method is useful to check that the measured viscosity ratios are correct where no other experimental data are available and for trouble shooting the experiments.

Experiments

The experimental apparatus is based upon apparatus reported by Russell et al. (2003). A detailed schematic flowsheet of the apparatus is shown in Figure 4. The apparatus adopts a two-sided arrangement similar to that employed in gas chromatography. The pressure changes are measured differentially between the measurement gas flow and a reference gas flow. Any effects due to transient variations in flow and pressure are unseen by the pressure transducer because they affect both sides equally. A flow setting block has been designed to provide four equal flow streams, one measurement flow, one reference flow and two purge flows After the flow setting block a small perturbation flow is added to the measurement side of the apparatus at valve 3-PSV-3. Two delay lines which separate the flow and viscosity pressure affects connect the two main flows to opposite sides of the pressure transducer. A *Furness* differential, pressure transducer DPT is used to measure the pressure changes. Downstream of the pressure transducer an additional pair of delay lines followed by the flow sensing capillaries are mounted inside cold aluminum block. To ensure thermal stability, the capillaries are wound onto a nickel core. The aluminium block is cooled directly by a peltier

chiller and is insulated with 50 mm of polyurethene foam. After the capillaries all flow streams are joined together and vent via a dome-loaded back pressure regulator.

Each experiment lasts about 40 minutes and involves recording the pressure changes for first adding the perturbation flow and then removing it in a single datafile. This method was adopted to enable the 'remove' perturbation pressure change sequence to be used as a check on the 'addition' perturbation data for constant conditions.

Viscosity gradients were measured for mixtures of helium–HFC-125 at ± 23 °C using gases supplied by BOC. The helium was supplied as 99.99% purity and the HFC-125 as 99.0% purity. Measurements were made at both temperatures using small perturbation flows of each pure gas to perturb main flow compositions at nominal 0.1 mole fraction intervals across the composition range. A second set of data using large perturbation flows of each pure gas to perturb main flow of the second component at 23°C.

Results

Two Consistency Tests can be applied to the binary mixture results for small perturbation flows. Test 1 examines the difference between the viscosity gradients $\left(\frac{\Delta \ln \mu}{\Delta X_i}\right)_{add} - \left(\frac{\Delta \ln \mu}{\Delta X_i}\right)_{rem}$ In the absence of errors these gradients *should* be the same. Because the *same* main gas and perturbation gas compositions are used, any differences in this test give a check on the precision of the measurement of the pressure changes.

Figure 5 gives the results for consistency Test 1 for measurements made at 23 °C. The differences between the gradients obtained for adding and removing the perturbation flow were in the range ± 0.01 and show a systematic bias. This behaviour has been observed before with mixtures of helium-argon (Russell et al 2003b). This systematic bias is caused by density differences between the measurement and reference flows. When the perturbation flow is added the gas mixture density (mass) is changed. If the flow paths in the apparatus are not in the same horizontal plane for both sides of the apparatus, small pressure changes (buoyancy) will be seen. The error observed is 3 times greater than that seen for helium-argon which is similar to the increase in density when HFC-125 is used. We conclude that the result for test 1 is acceptable but less satisfactory than previous measurements.

Test 2 compares the viscosity gradients at a set main–flow composition measured using each perturbation gases. The viscosity gradients for each perturbation gas cannot be compared directly because they are at slightly different compositions. This is because each gradient is at a slightly different composition $X_i^0 + 0.5\Delta X_i$ and ΔX_i depends on the composition of the perturbation gas used. Nevertheless all gradients measured should lie on the same curve of viscosity gradient against composition. The extent to which they diverge from a smooth curve depends on the precision of the pressure measurements and the error in the gas compositions.

The results for consistency Test 2 for both temperatures are present in Figure 6 . All gradients lie on common curves thus test 2 is satisfied for both temperatures. The shape of the gradient curve is complex with a clear maximum occurring at very high (≈95%) helium concentrations. The data have been fitted by least squares to a twelfth order polynomial. This high order polynmial was the simplest equation found to give an adequate fit of the data.

Viscosity gradients are of limited practical use, integration of the gradients to produce viscosity ratios are of far more interest. The poly nomial fitted to the gradient data for Test 2 is easily integrated to produce the viscosity ratios. The mixture viscosities relative to the viscosity of helium at 23 °C and -23 °C are plotted for both data sets in Figure 8. The pure

component ratios calculated from the small perturbations are $\frac{\mu_{He}}{\mu_{HFC-125}}$ = 1.4463 at 23 °C and 1.5284 at -23 °C These can be compared directly with values calculated from literature sources using pure component viscosities for helium taken from Toloukian (1975) and for HFC-125 Takahashi et al (1999). We have calculated the ratios should be 1.5311 at 23 °C and 1.6180 at -23 °C. There are significant differences between our results and the literature values The discrepancy has arisen because the HFC-125 used in these experiments contains impurities. A mass spectrometer has been used to analyse the composition of the suva-125. The results of the analysis show that the gas contains at least 1.5% nitrogen, 1.5 % oxygen and a small amount of gaseous water.

To confirm that the ratios were correct for the gases used a series of large perturbation measurements were made at 23°C. These results are shown in Figure 7 and agree well with the small perturbation data suggesting the data are correct but subject to a systematic error produced by the presence of the contaminents.

Conclusions

We have developed a new capillary viscometric technique based on making differential measurements. The technique and apparatus have been shown to work for non ideal gas mixtures. Careful design of the apparatus permits effects arising from volumes of mixing and thermal expansion to be compensated for to produce high accuracy viscosity ratios. By the use of internal consistency checks it has been shown that the apparatus produces viscosity gradient data of high quality. The method is relatively fast, simple and has the potential to work at much higher pressures

Notation

G logarithmic viscosity gradient
m molar flow rate of perturbation gas
M molar flow rate of main-flow gas
P_0 pressure at gauge before perturbation flow added
P_1 pressure at gauge after perturbation flow added
P_2 pressure at gauge after viscosity change has occurred
P_3 pressure at gauge after perturbation flow removed
P_4 pressure at gauge after viscosity change has occurred
Q volumetric flowrate of main flow
q volumetric flowrate of perturbation flow
R ratio of viscosity pressure change to flow pressure change
T temperature
$\overline{V}$ molar volume
X mole fraction

Greek symbols

μ viscosity
Δ a small but finite difference

subscripts

He helium
Suva-125 Suva-125
i species i
add adding perturbation
rem removing perturbation

calc value calculated from polynomial fitted through all measured gradients

superscripts

0 main flow gas

T perturbation gas

References

Heslop, M. J., G. Mason, and B. A. Buffham, Institution of Chemical Engineers Research Event, Newcastle. Paper No227. CD-ROM Record Nos 13,098-13,161. (1998)

Mason, G., B. A. Buffham, M. J. Heslop, and B. Zhang. *Chem. Engng. Sci.*, **53** 2665 (1998)

Mason G., B. A. Buffham, M. J. Heslop, P. A. Russell and B. Zhang. *Chem. Engng. Sci.*, **55** 5747 (2000)

P. A. Russell , B. A. Buffham, Mason G. and M. J. Heslop, Accepted for publication AIChE Journal (2003a)

P. A. Russell , B. A. Buffham, Mason G. and M. J. Heslop, To be published (2003b)

P. A. Russell, B. A. Buffham, G. Mason and K. Hellgardt. fifteenth symposium on thermophysical properties Boulder Colorado USA(2000c)

Touloukian Y. S., S. C. Saxena and P. Hestermans “Viscosity” Thermophysical properties of matter. The TPRC data series, Vol 11, Plenium, New York, (1975)

Takahashi M., Shibassaki-kitakawa N., and C. Yokoyama, *Int. J. Thermophys*, **20**:2 (1999)

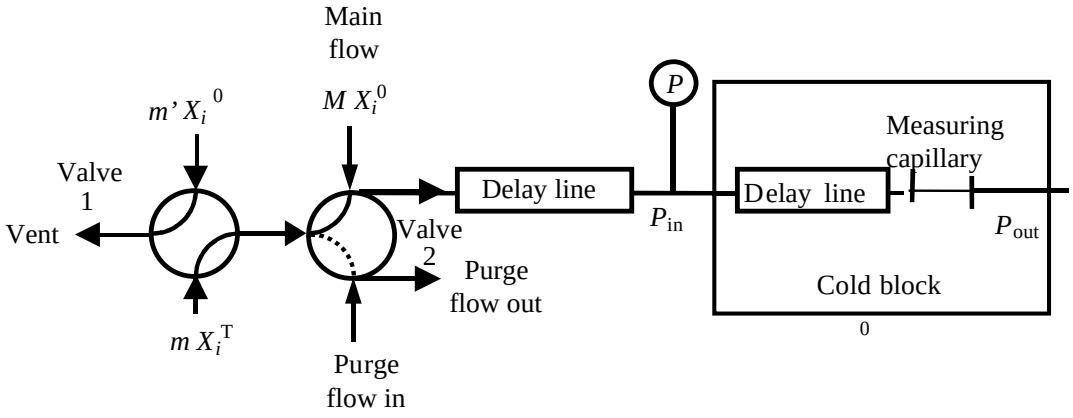

Figure 1 Diagram of the new non-ideal gas apparatus. In normal operation a (main) flow of gas, M of known composition X_i^0, flows through valve 2 then an ambient temperature delay line (low resistance empty tube), a cold delay line and finally the measuring capillary tube. In an experiment a small perturbation flowof composition X_i^T is added to the main flow and the responses are observed at the pressure gauge. Further measurements are made when the perturbation flow is removed.

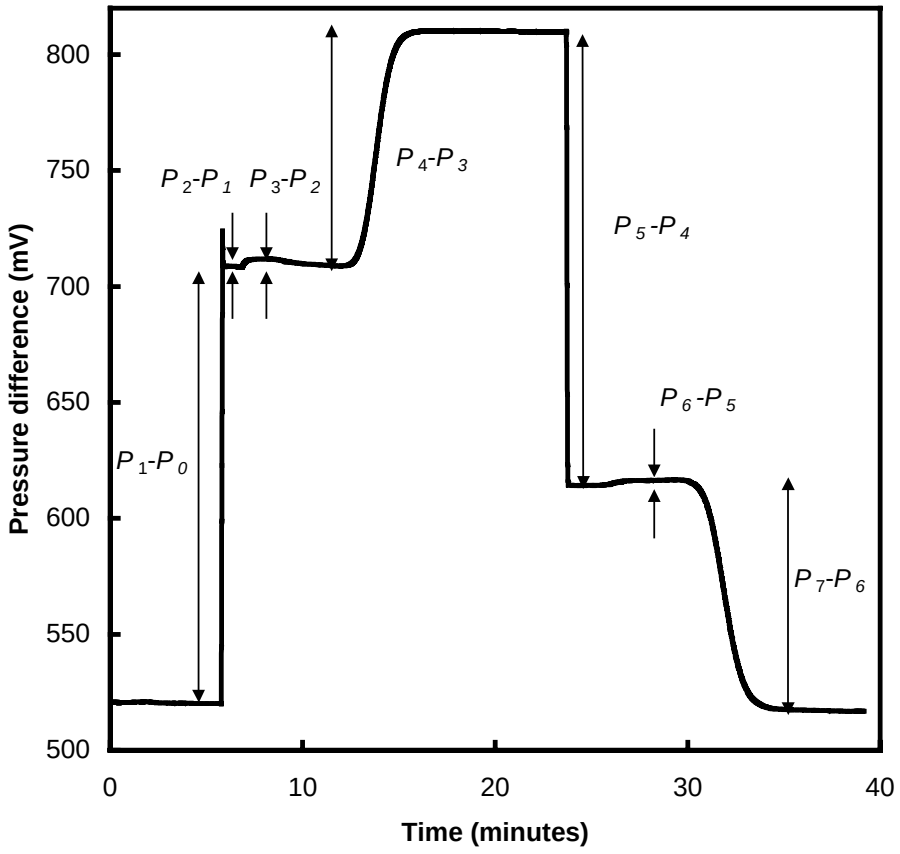

Figure 2 The actual pressure record for an experimental run at 23 °C where a perturbation flow of HFC-125 was added to, then removed from a helium main gas flow. The pressure changes are: Step1 P_0 to P_1 due to increase in flow when perturbation is added; Step2 P_1 to P_2 Volume change on mixing of the two gas flows; Step3 P_2 to P_3 Change in thermal expansivity of gas in cold block; Step4 P_3 to P_4 increase in viscosity due to increase in helium mole fraction; Step5 P_4 to P_5 decrease in flow when perturbation is removed; Step6 P_5 to P_6 Change in thermal expansivity of gas in cold block; Step7 P_6 to P_7 increase in viscosity due to decrease in helium mole fraction

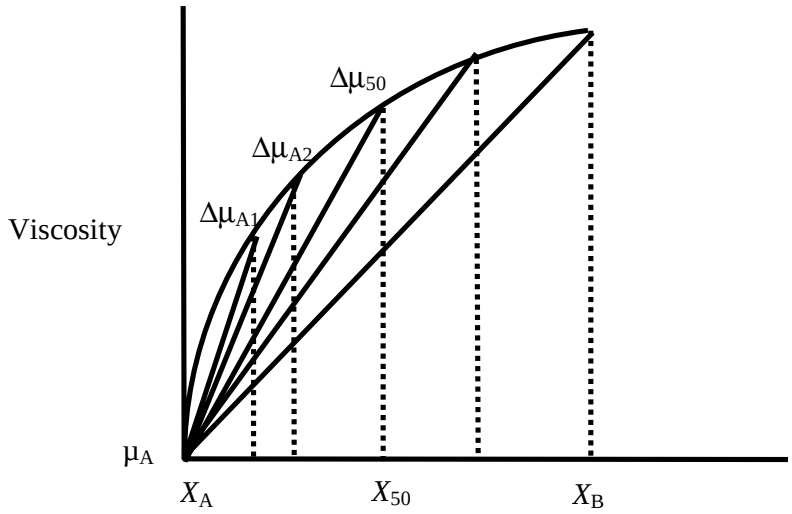

Figure 3 Diagram showing how the composition is changed by increasing the flowrate of the perturbation used.

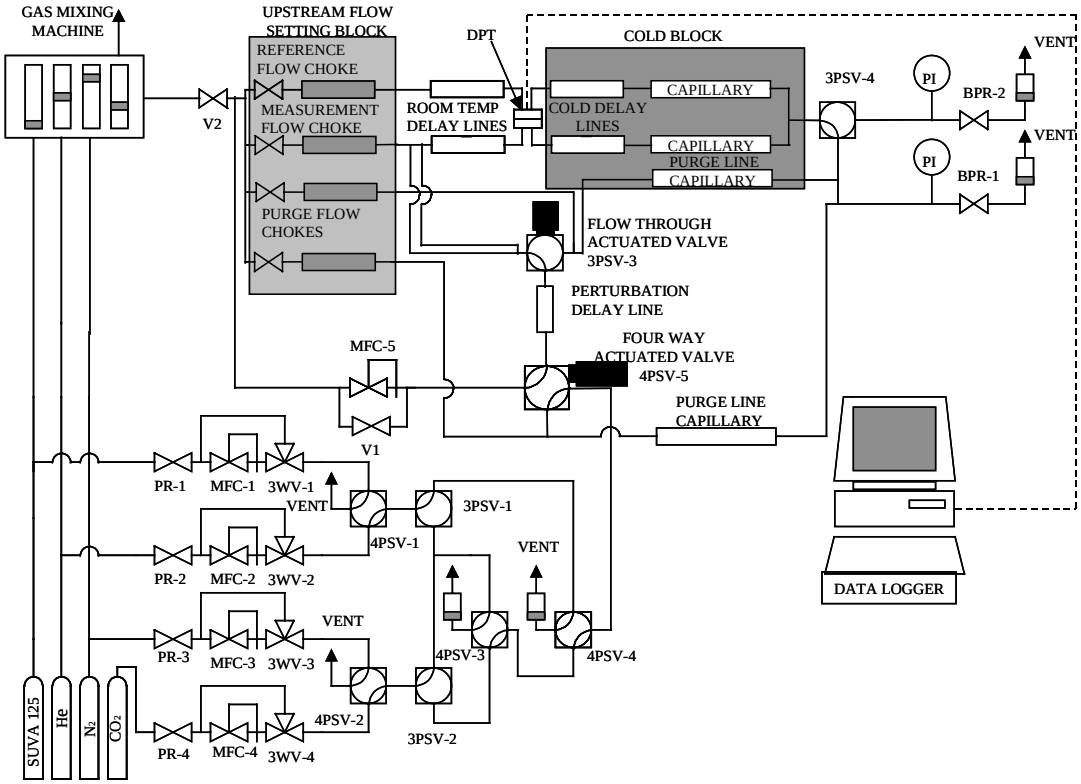

Figure 4 Schematic flow diagram of new experimental apparatus. BPR-1, BPR-2 and BPR-3, Modified back pressure regulators based on *Porter Instruments* 9000; DPT , *Furness Controls* FCO 40 differential pressure transducer; MFC-1,MFC-2, MFC-3 and MFC-4, *Porter Instruments* VCD 1000 flow controllers PR1,PR2,PR3 and PR4, modified *Porter Instruments* 8286 pressure regulators; 3PSV-1, 3PSV-2, 3PSV-3 and 3PSV-4, *Valco* UWE three port switching valves; 4PSV-1, 4PSV-2, 4PSV-3, 4PSV-4 and 4PSV-5, *Valco* UWE three port switching valves; 3WV-1, 3WV-2, 3WV-3 and 3WV-4, *SSI* 02-0182- , Swagelok series 40 ball valves: V1 and V2

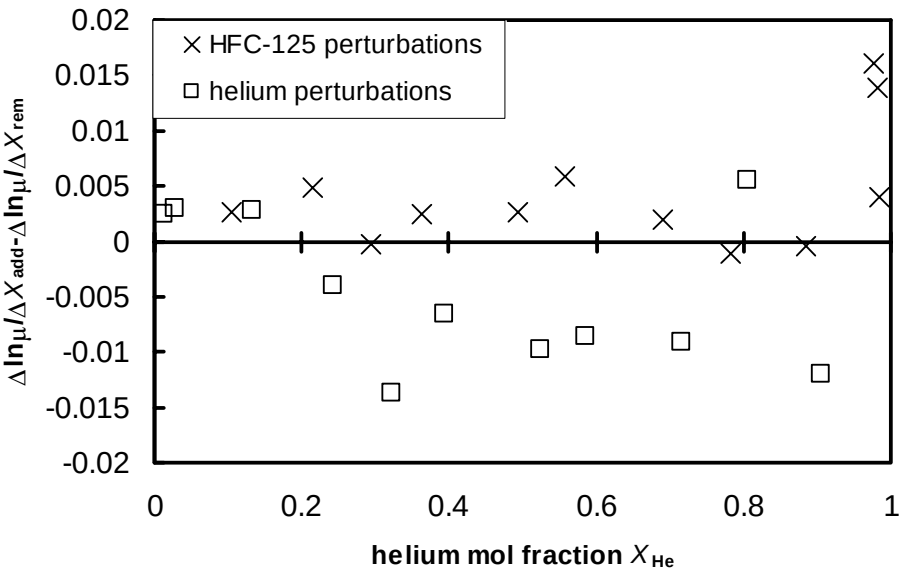

Figure 5 Errors in the data set are illustrated for the mixture helium–HFC-125 using a graph of the difference $\frac{\Delta \ln \mu}{\Delta X}_{\text{add}} - \frac{\Delta \ln \mu}{\Delta X}_{\text{rem}}$ versus helium mole fraction at -23 °C. Note the systematic bias of results the helium perturbations are predominantly negative and the HFC-125 are positive. This is due to high density difference between the components of the mixture .

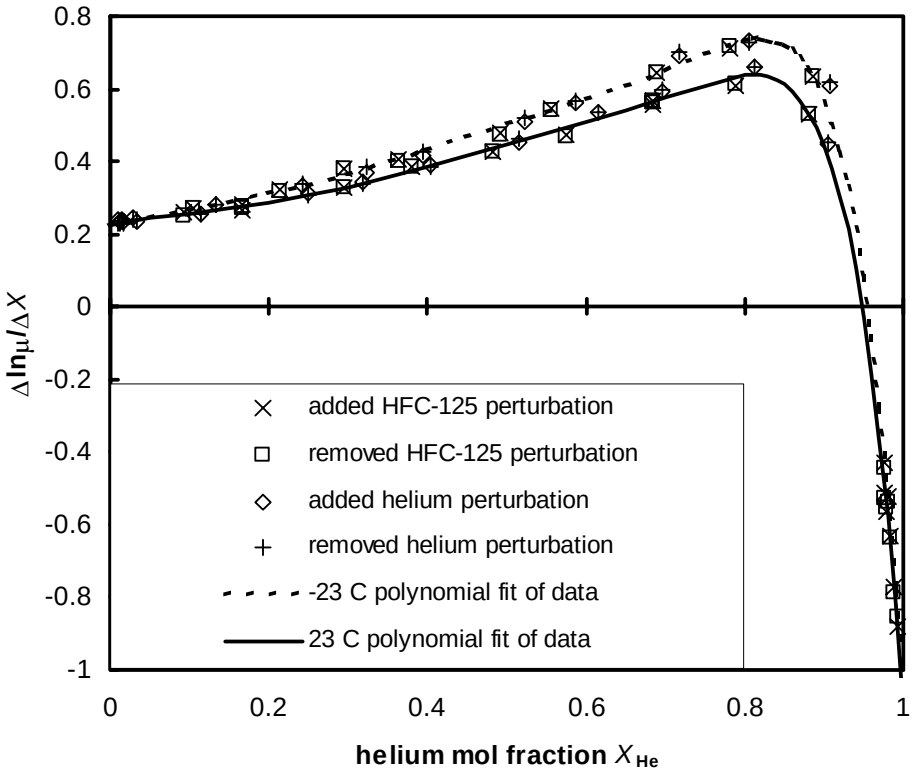

Figure 6 The second consistency test of the data is applied by plotting of $\Delta \ln\mu/\Delta X$ versus helium mole fraction for all experimental measurements made on the mixture helium–HFC

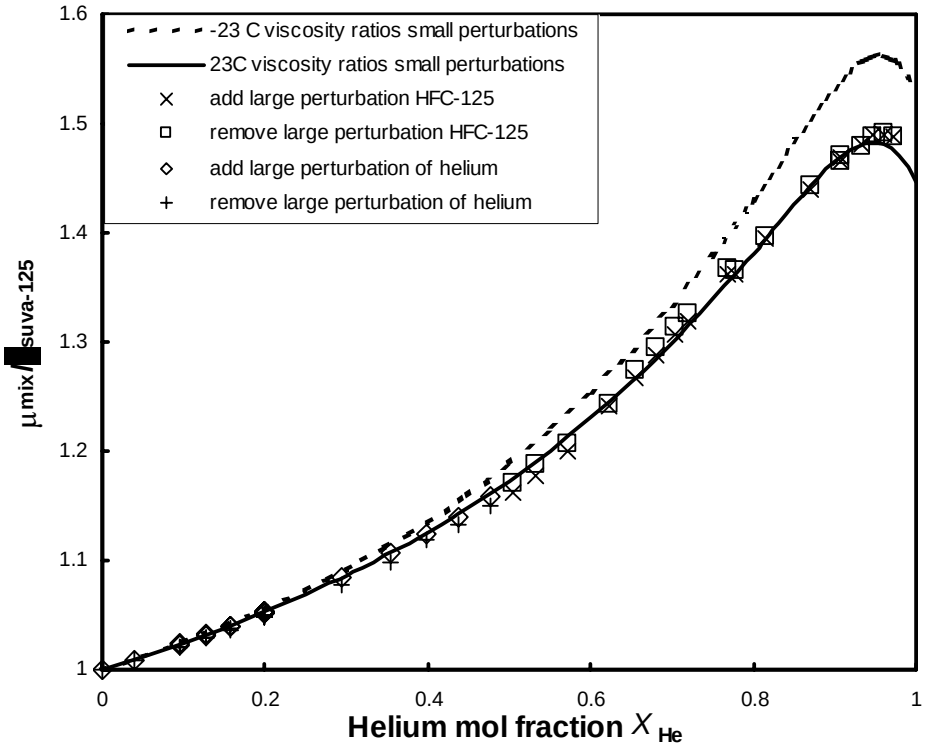

Figure 7 The viscosity ratios for mixtures of helium–HFC-125 at ±23 °C .Produced by integration of fitted polynomials. Data points refer to results obtained directly using large perturbation method.